Liquid Crystals
Publication details, including instructions for authors and subscription information:
http://www.informaworld.com/smpp/title~content=t713926090

Anchoring transition and influence of director fluctuations in liquid crystal droplets

G. Sai Preeti[a]; N. Satyavathi[b]; K. P. N. Murthy[a]; V. S. S. Sastry[a]
[a] School of Physics, University of Hyderabad, Hyderabad, India [b] Department of Physics, Osmania University, Hyderabad, India

Online publication date: 14 December 2009

To cite this Article Sai Preeti, G. , Satyavathi, N. , Murthy, K. P. N. and Sastry, V. S. S.(2009) 'Anchoring transition and influence of director fluctuations in liquid crystal droplets', Liquid Crystals, 36: 12, 1379 — 1388
To link to this Article: DOI: 10.1080/02678290903217424
URL: http://dx.doi.org/10.1080/02678290903217424

Liquid Crystals,
Vol. 36, No. 12, December 2009, 1379–1388

Taylor & Francis
Taylor & Francis Group

Anchoring transition and influence of director fluctuations in liquid crystal droplets

G. Sai Preeti[a]*, N. Satyavathi[b], K.P.N. Murthy[a] and V.S.S. Sastry[a]

[a]*School of Physics, University of Hyderabad, Hyderabad, India;* [b]*Department of Physics, Osmania University, Hyderabad, India*

(Received 1 April 2009; accepted 28 July 2009)

Micro-droplets of nematic liquid crystals have been investigated under radial boundary conditions, based on a lattice model which incorporates explicitly the elastic properties of the medium as variable parameters in the Hamiltonian. Equilibrium director configurations have been simulated, employing the Monte Carlo technique, as a function of anchoring strength ε_S at the spherical boundary surface. A very sharp transition from a uniaxial nematic structure to a radially ordered state results in ε_S being increased beyond a threshold. The flexibility offered by this Hamiltonian is utilised to investigate this structural transition as a function of the splay elastic coefficient K_1. The results indicate several features: (1) the transition is as expected influenced by K_1; (2) the transition seems to be mediated by a process of complete wetting by the outer spherical surface, except for the small uniaxial core region sustained by the elastic energy penalty otherwise incurred; (3) the degree of splay contribution has multiple effects on the transition including changes in the critical anchoring strength at the transition, and the nature of the transition itself; (4) profiles of the director fluctuations across the (concentric) spherical layers indicate evidence of frustration caused by the competing interactions generated in the system due to the boundary conditions imposed.

Keywords: polymer dispersed liquid crystal droplet; Monte Carlo simulations; elastic potential

1. Introduction

Polymer dispersed liquid crystals (PDLCs) are a class of materials that are very important from the point of view of applications (*1–3*). The electro-optic properties, for example, have been studied extensively as a function of external parameters such as the applied voltage (*3–5*). Holographic PDLCs are a subgroup of these materials, and are equally important for display devices (*6, 7*). Molecular organisations in these materials due to the different host materials have attracted the attention of physicists (*8*).

Experimental techniques such as ^{2}H nuclear magnetic resonance (NMR) and polarisation methods are used to study these materials. The effect of molecule size (*9*) and anchoring due to the substrates (*10*) have been studied using NMR techniques. The NMR spectra have been interpreted by simulation using Monte Carlo (MC) methods (*11*) and also by different phenomenological models (*12*). These systems have been investigated using mean field methods (*13–15*), and analysed based on Landau theory (*16*).

In particular, these droplets of micrometre size, or less, have been investigated (*16*) under different anchoring conditions imposed by the bounding polymer matrix. The motivation for these studies originated both from basic issues involved in determining the equilibrium structures in such soft model systems under confinement, as well as from their applications as optical modulators (*17, 18*). Of specific interest is a droplet subjected to radially ordering conditions at the polymer–substrate interface (*19*). Markov chain MC studies based on the Lebwohl–Lasher (LL) model (*20*) show that the droplet, in its nematic phase and under strong anchoring conditions, is essentially radially ordered but for a small spherical region at the core, which has uniaxial nematic phase (*21*). The origin of this core region is attributed to the delicate balance between the energy penalty imposed by the radial ordering (at that curvature) and the energy expenditure involved in maintaining an interfacial spherical region (between the inner uniaxial ordering and outer radial ordering (*11*)). Obviously, this is dictated, on the one hand, by the degree of relevant elastic distortion sustainable (in this case the splay distortions) *vis-á-vis* the influence of the intermolecular interactions to bring about uniaxial ordering, on the other. Earlier simulations (*22*) based on the LL model have clearly shown that the size of this inner uniaxial core is independent of the actual size of the droplet (assuming that it is always bigger than the core region) (*23*), and it is essentially determined by the nature of the Hamiltonian chosen. To make this scenario quantitative, the concept of the radial order parameter S_R was introduced to specify the degree of alignment of the liquid crystal region along the radial direction of the droplet, along with S which denotes the uniaxial ordering of the nematic phase (*22*). These simulations focused on the temperature dependence

*Corresponding author. Email: gsaipreeti@yahoo.com

ISSN 0267-8292 print/ISSN 1366-5855 online

DOI: 10.1080/02678290903217424
http://www.informaworld.com

of the formation of the radial order, and its propagation to the inner layers, as the nematic phase is formed. Further studies were carried out on these droplets to understand the effects of applied external field (*21*) at various anchoring strengths at the polymer interface. Different molecular organisations were investigated by illustrating their influence on the simulated NMR spectra. Droplets with toroidal and bipolar boundary conditions were also studied using MC simulations for different anchoring strengths and at different external fields (*19, 24–26*). More recently, a droplet of biaxial molecules was investigated using MC simulations based on a suitable lattice Hamiltonian (*27*) for the different kinds of defects formed in such systems (*28*).

One of the interesting questions that arises in this connection concerns the role of the anchoring strength of the bounding surface in inducing radial order (at a given temperature in the nematic phase), and the nature of the transition from a wholly uniaxial structure (when the bounding surface is completely ineffective in influencing the liquid crystal inside) to an essentially radial structure, as was observed in the earlier work under strong anchoring conditions. The other important considerations include the role of the relevant elastic property (splay energy represented by the corresponding coefficient K_1) in determining the nature of this transition, the size of the inner uniaxial core that emerges, and also the extent of competition that it may provide at the interfacial region, betrayed by the fluctuations in the order parameters quantifying the equilibrium structure of the medium. In other words, use of a suitable Hamiltonian which can incorporate the elastic properties of the medium while accounting for the nematic order of the liquid crystal would be very appropriate in the study of this problem. One of the questions addressed is whether the influence of the anchoring by the surface, and consequent induced radial order, could be viewed as due to a wetting phenomenon.

In this context, it may be noted that a lattice-based Hamiltonian which explicitly takes into account the elastic properties of the medium via the three elastic coefficients (splay (K_1), twist (K_2) and bend (K_3) elastic constants) is used for this study. This interaction is computed for nearest-neighbour lattice elements. Its application to the Schadt–Helfrich cell has been demonstrated through detailed MC simulations (*29*). In this work, we shall adopt this model to study the equilibrium director configurations of a PDLC droplet in its nematic phase under radial boundary conditions, with specific focus on the anchoring transition induced by variable coupling to the polymer matrix, and the role of splay distortion.

2. Model used

The director configuration of a system with given geometry and boundary conditions is determined by minimising the elastic free energy of the sample in the continuum limit. The corresponding energy density in the nematic phase is expressed in terms of powers of the gradient of the director **n**, restricting to only the quadratic terms, as

$$\Psi = \frac{1}{2}\{K_1(\nabla.\mathbf{n})^2 + K_2[\mathbf{n}.(\nabla \times \mathbf{n})]^2 + K_3[\mathbf{n} \times (\nabla \times \mathbf{n})]^2\}. \quad (1)$$

Only very simple systems permit an analytical solution of the above equation and, very often in practice, free energy is calculated through numerical procedures. An alternative method is to assume a lattice model of pairwise interacting nearest-neighbour elements stipulated by a model Hamiltonian, and to construct an equilibrium ensemble at different reduced temperatures (measured in units of the interaction strength introduced in the Hamiltonian), employing the usual Markov chain MC methods (*30*) based on the Metropolis algorithm. Earlier work on these droplets based on this methodology using the LL model was limited by the fact that the interaction energy depends only on the relative orientation of the two particles but not their relative positions, and hence cannot distinguish between the different deformations. This potential thus corresponds to an assumption of equal elastic constants (the spherical approximation).

An alternative approach, initiated by Gruhn and Hess (*31*), and later developed by Romano and Luckhurst (*32*), involves derivation of a model potential for a pairwise additive interaction between local directors, which approximately reproduces the elastic free energy density of the system. This is achieved by mapping the above equation onto a suitable expansion of the interaction potential. In this scheme, the space is discretised to a cubic lattice, each site representing a director. The free energy of the system is defined as the sum of pairwise additive interactions between nearest-neighbouring sites. An expression, with appropriate multiplicative and additive constants chosen to scale the isotropic average of the energy to be zero, is then derived to be used as the model potential for MC simulations. These naturally are defined through specific combinations of the three elastic coefficients, thereby making the model rich and useful so as to be applicable to real systems with differing elastic constants. Derivation of the potential used in this work is briefly outlined below, in order to introduce the notation.

The pair potential between two directors located at two neighbouring sites, say j and k, is expanded in terms of a complete set of basis functions depending on the orientation of the two directors $\mathbf{n}_j$ and $\mathbf{n}_k$ and the orientation of the vector joining them $\mathbf{r}$. The S-functions (*29*) $S_{L_j,L_k,J}(\mathbf{n}_j, \mathbf{n}_k, \mathbf{r})$ were found to be suitable for this purpose. Here the index L_j refers to the jth director, L_k to the kth director and J corresponds to the inter-director vector, taking values from $(L_j + L_k)$ to $|L_j - L_k|$. In this particular application it was found that the S-functions depend only on the scalar invariants associated with the vectors in their argument, viz. $a_j = \mathbf{n}_j.\mathbf{r}$, $a_k = \mathbf{n}_k.\mathbf{r}$, $b_{jk} = \mathbf{n}_j.\mathbf{n}_k$ and $c_{jk} = \mathbf{n}_j.(\mathbf{n}_k \times \mathbf{r})$. The symmetry of the nematic phase which requires that $\mathbf{n} = -\mathbf{n}$ demands that the total rank, $(L_j + L_k + J)$, of the S-function be even, thereby eliminating the factors c_{jk}. Thus, the pair potential between two neighbouring sites j and k is expanded in terms of S-functions restricted to terms of even total rank, with suitable coefficients, as (*29, 33*)

$$\Phi_{jk} = \sum_{L_j,L_k,J} \varphi_{L_j,L_k,J} S_{L_j,L_k,J}(a_j, a_k, b_{jk}). \tag{2}$$

This pair potential is then mapped onto the expression for the free energy density, assuming small angular displacements of the director so as to replace the gradients by finite increments. Finally, certain well-defined deformations are considered in both the pair potential and the initial free energy density (approximated for small deviations), so as to derive the relation between the coefficients of expansion in the pair potential and the elastic constants. The final expression for the pair potential $\Phi_{L_j,L_k,J}$ is given by

$$\begin{aligned}\Phi_{jk} = {} & \lambda\left[P_2(a_j) + P_2(a_k)\right] + \mu\left(a_j a_k b_{jk} - \tfrac{1}{9}\right) \\ & + \nu P_2(b_{jk}) + \rho\left[P_2(a_j) + P_2(a_k)\right] P_2(b_{jk}).\end{aligned} \tag{3}$$

Here, P_2 is the second-rank Legendre polynomial. The coefficients of expansion are related to the elastic constants through the following relations, involving the chosen linear dimension Λ of the volume element in the cubic lattice to represent their local directors:

$$\begin{aligned}\lambda &= \tfrac{1}{3}\Lambda(2K_1 - 3K_2 + K_3), \\ \mu &= 3\Lambda(K_2 - K_1), \\ \nu &= \tfrac{1}{3}\Lambda(K_1 - 3K_2 + K_3), \\ \rho &= \tfrac{1}{3}\Lambda(K_1 - K_3).\end{aligned} \tag{4}$$

An interesting feature of this potential is that Λ enters as a length scale over which the director gradient is discretised and defines the lattice parameter corresponding to the distance between the neighbouring sites. By setting all the elastic constants equal to each other, say K, the above potential is reduced to the form of the LL potential,

$$\Phi_{jk}^{LL} = -\epsilon P_2\left[\cos(\mathbf{n}_j.\mathbf{n}_k)\right]. \tag{5}$$

Under these special conditions, the energy scale parameter ϵ is equal to ΛK for the present model. In general, the total free energy of the system is then given by

$$\Psi = \frac{1}{2}\sum_{j=1}^{N}\sum_{k=1}^{6}\Phi_{jk}, \tag{6}$$

where N is the number of sites. Following the procedure adopted earlier, the scaled potential for use in simulations is obtained by dividing Equation (3) by $|\nu|$. This leads to a scaled temperature, to be used in the MC scheme, given by

$$T^* = k_B T/|\nu| = 3k_B T/(\Lambda|K_1 - 3K_2 - K_3|). \tag{7}$$

3. Details of simulations

Within the framework of the above lattice Hamiltonian model (Equation (3)), the surface anchoring effects due to confinement on the liquid crystal medium are accounted for by including an appropriate additional layer of surrounding lattice sites, hosting mesogenic units with fixed orientations that are compatible with the stipulated boundary conditions. These are sometimes referred to in the literature as ghost sites (*22, 26*), and they do not participate in the MC simulation. Earlier application of this Hamiltonian to study field-induced transitions in the Schadt–Helfrich cell (*29*) introduces the surface anchoring effects through this construct. We adopt the same procedure here to simulate the anchoring effects at the surface of the liquid crystal droplets. To this end, a sufficiently large cubic lattice is considered and a sphere of chosen radius (in lattice units) is carved out (*21*). Consequently, the bounding surface will be a jagged sphere due to the discrete nature of the arrangement of lattice points. Each lattice point is associated with a local director, say, spin averaged over molecules enclosed in the cubic volume element of dimension Λ. Each spin is associated with a unit vector oriented along that local director. The lattice sites inside the sphere represent local directors within the liquid crystal which participate in the MC chain dynamics, while those outside the sphere with fixed desired orientations correspond to a substrate imposing the required boundary conditions (in the present case, oriented towards the centre so as to impose radial boundary

condition surface anchoring). These fixed molecules, representing the substrate, hence do not participate in the simulation moves.

The flexibility of this Hamiltonian is utilised to study the effect of elastic properties on the director distribution by taking the example of a liquid crystal with known elastic constants in the nematic medium for purposes of simulation in this work. Thus, we set the values of K_1, K_2 and K_3 from the measurements on p-azoxyanisole (PAA) taken at a reduced temperature T/T_{NI} equal to 0.963 as 7.0×10^{-12} N, 4.3×10^{-12} N and 17.0×10^{-12} N, respectively (*33*). The energy scale is set, for a given set of elastic constants, by the dimension of the volume element over which the local director is defined, and hence the effective temperature at which the canonical ensemble is constructed is determined by this choice of Equation (7). From the previous studies on planar hybrid film (*29*) it was concluded that the continuum results could be recovered for a choice of this dimension typically in the range of a few hundred angstroms and above, corresponding to a typical reduced temperature T^* of 0.10 and below. Assignment of lower values of Λ, leading to higher values of T^*, would correspond to, in physical terms, appreciable fluctuations in the director field. It was found that, for such effective high temperatures, the predicted results were not consistent with the expected behaviour from continuum theory based on minimisation procedures. A typical value for Λ above which the fluctuations are small enough to yield satisfactory simulated results consistent with experimental results was reported to be around 700 Å.

Due to the symmetry of the problem (a nematic droplet subjected to radial boundary conditions) only splay distortion is operative, and this convenient situation is exploited by extending these studies as a function of the relative splay energy contribution, effective by varying the value of K_1 relative to the other elastic constants. To this end, the simulations are performed for different K_1 values at fixed K_2 and K_3, and the results are then discussed for convenience in terms of the ratio (called the scale factor, say α) of the assigned K_1 value to its actual value.

These studies are also aimed at examining the influence of the surface anchoring on changes in the director structure, and accordingly we introduce a variable anchoring strength ε_S (in units of the energy scale set above), ranging from 0 to 1. This defines the strength of interaction between the liquid crystal molecules and the (orientationally) fixed molecules in the substrate. Introduction of this variable facilitates a study of possible anchoring-induced structural transitions in the system.

Different physical properties are computed based on these simulations, and in order to get an insight into the director structure inside the droplet, we consider the droplet to comprise of concentric shells of a given width, indexing them in ascending order as we move away from the centre of the droplet. We report ensemble averages of different properties measured within each of the layers. The variables so computed include: uniaxial orientational order S_A (referred to the axial order in the system), the radial order S_R (measuring the degree of alignment of liquid crystal molecules along the radial direction in the droplet, computed from $\langle P_2(\cos(\theta_i))\rangle$ where θ_i is the angle made by each of the liquid crystal molecules in the droplet with respect to the local radial direction and the angular brackets represent the ensemble average over the sample as well over the MC runs), root mean square (RMS) fluctuations in these orders within each concentric layer, and the rigid lattice limit NMR spectrum of deuterium (located on the core of the molecule) expected from the system assuming that the Zeeman field is always applied parallel to the instantaneous director. We take known typical values for the deuterium quadrupole coupling constants (175 kHz) and the C–D bond angle with respect to the long axis of the molecule (60°).

Canonical ensembles at the fixed reduced temperature of 0.01 (corresponding to K_1, K_2 and K_3 values of 7.0×10^{-12} N, 4.3×10^{-12} N and 17.0×10^{-12} N, respectively, and $\Lambda = 710$ Å) were constructed for a droplet with a radius of 15 lattice units using the Markov chain MC-simulation-based Metropolis algorithm. The data for computation of the variables of the above physical properties were collected over 5 million MC steps after ignoring the first 1 million steps for equilibration. The results are discussed below.

4. Results and discussion

With the scale factor fixed at unity (i.e. using the typical values of the elastic coefficients of PAA as such), we see an anchoring mediated structural transition of the director configuration as depicted in Figure 1. Both S_A and S_R show a sudden jump at $\varepsilon_S \sim 0.54$. When ε_S is close to zero, the surface does not have a significant influence on the director structure and the droplet has a predominantly uniaxial director configuration represented by a high value of S_A, and the corresponding S_R is low. As the value of ε_S is increased the uniaxial order decreases and at the threshold value of about 0.54 the axial order practically vanishes, while the radial order assumes a value very near unity. This would physically correspond to an anchoring-mediated sudden change in the director structure finally culminating in an essentially radially ordered director configuration. These results are consistent with those of the earlier work carried out with

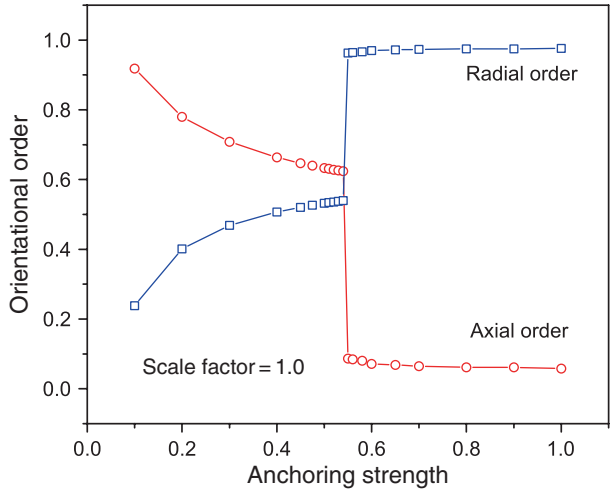

Figure 1. Variation of radial and axial order with anchoring strength for a scale factor 1.00.

the LL model with $\varepsilon_S = 1$. It is interesting to see the corresponding changes in the layer-wise order parameters as a function of ε_S. These are depicted in Figures 2(a) and 2(b). Both of the figures, which are complementary, indicate that below the threshold ε_S the development of radial order, at the expense of the axial counterpart, is gradual as one moves out from the centre of the droplet, and the droplet is thus becoming gradually transformed from a pure uniaxial symmetry to a more spherical symmetry. Just at the threshold value, a sudden transition of the director structure takes place, making it essentially spherically symmetric, but for a small inner core (of a radius of about 3 to 4 lattice units) which still manages to have uniaxial order. This, is due to the significant elastic energy involved in forcing the radial orientations of the director to the very centre of the droplet (*19, 34*). Thus, the minimum free energy is obtained by allowing a small core of the uniaxial region with some energy cost at the interface between two differently ordered regions of the medium.

Figure 3 shows the RMS value of layer-wise (uniaxial) order fluctuations as ε_S is varied from 0.1 to 1.0. These fluctuations seem to provide an insight into the progression of the radial order towards the centre, and are significant near the interfacial region at the delimiting surface due to frustration effects. When ε_S is low (0.1) the effect of radial anchoring seems to make the axial order fluctuate progressively more, as the confining surface is reached from the centre. At $\varepsilon_S = 0.2$, there are very significant fluctuations which persist typically in the outer five layers, implying that at this anchoring value the energy cost of percolating the radial order is competing with the interfacial energy (at the surface) involved to retain a large enough uniaxial region. It may be noted that this energy cost is relatively small at this large radius of the uniaxial droplet. However, further increase of ε_S to 0.3, and up to a threshold value of about 0.54, indicates rather curiously that the fluctuations are uniform over the layers, but for a small (approximately two-fold) increase in the middle layers of the droplet. This suggests that the uniaxial order fluctuations are smaller at the core (away from the

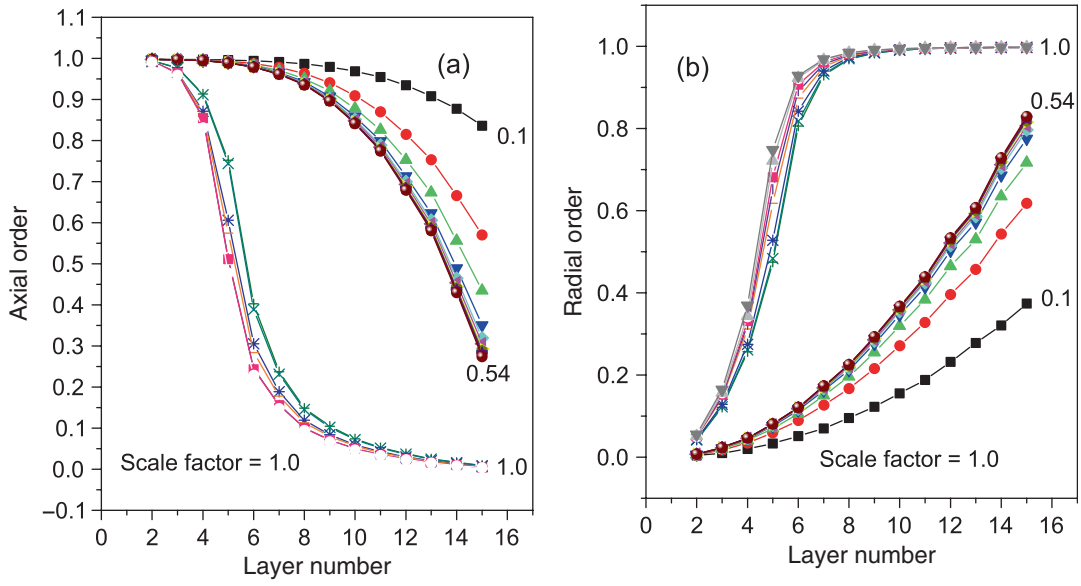

Figure 2. (a) Variation of radial order with layers for the scale factor 1.00 for different anchoring strengths (the different plots correspond to different anchoring strengths ε_S, as indexed). (b) Variation of axial order with layers for the scale factor 1.00 for different anchoring strengths (the different plots correspond to different anchoring strengths ε_S, as indexed).

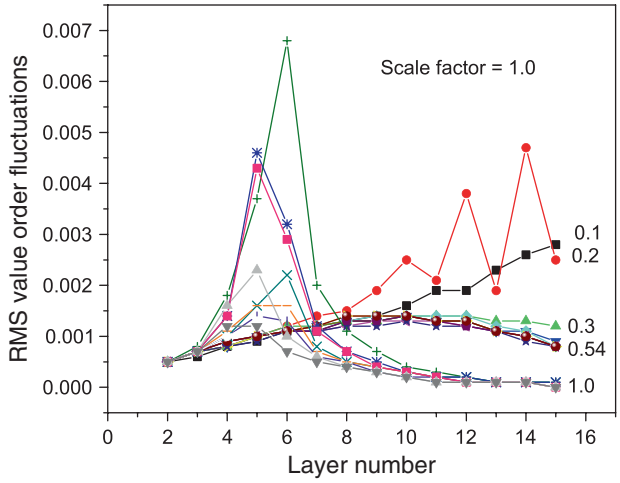

Figure 3. Variation of RMS value of order fluctuations with layer number for different anchoring strengths (the different plots correspond to different anchoring strengths ε_S, as indexed).

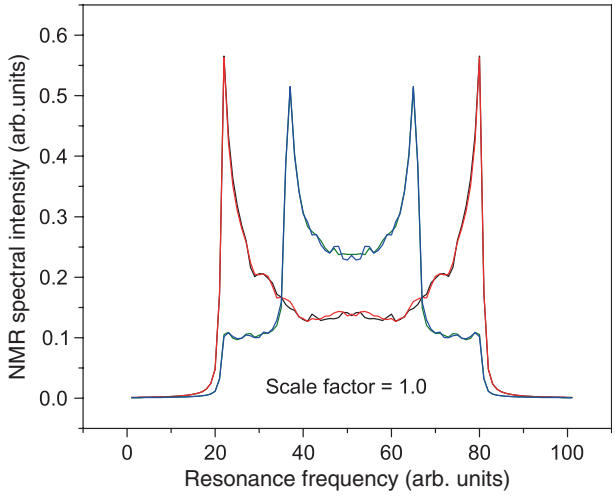

Figure 4. Simulated NMR spectrum for different resonant frequencies for the scale factor 1.00 (inner plot representing axial order).

competing boundary conditions) and at the surface (due to the pinning effect from the surface), and are somewhat more pronounced in the mid-layers, as can be expected under the circumstances. At the onset of the anchoring-induced transition, beyond the threshold value of ε_S, however, the scenario changes qualitatively. The order fluctuations suddenly shift towards an inner layer (around 4 to 5 units) and show systematic peaks (unlike the fluctuations near the outer layers at $\varepsilon_S = 0.2$) at the interfacial surfaces, their position shifting progressively to inner layers as the anchoring strength is increased to unity beyond the threshold value. These fluctuations unambiguously show the onset of radial order and its progression with anchoring strength, and provide the signature of the anchoring-induced structural transition in the medium. In order to correlate the above changes with experimentally observable quantities, ^{2}H NMR spectra expected from the different director configurations were generated for different ε_S values. Figure 4 shows two limiting spectra for $\varepsilon_S =$ 0.1 and 1.0.

The simulations were extended to find the effect of varying the energy costs of the relevant elastic distortion (i.e. the splay constant K_1 relative to its actual value, while retaining the other two elastic constants the same) through the scale factor α, as mentioned before. Figure 5(a) shows the variation of the two orders with ε_S as α is varied from 0.1 to 3.0 in some convenient steps. It may be noted that, after the onset of the anchoring-induced transition, the region of interface between the uniaxial core and the outer radial region depends on the balancing of the elastic energy costs involved, and in this case is determined by the splay elastic coefficient; other competing conditions are kept constant. Thus, Figure 5(a) shows that the effect of varying the relative value of the splay elastic constant is two-fold: the threshold value for the anchoring transition increases with increase of α, and the extent of change in one type of order to the other type after the anchoring transition decreases with α. This is consistent with the picture that, as K_1 is systematically increased, it requires more anchoring influence from the boundary to induce this transition, and a higher K_1 value also demands a larger uniaxial core for energy balance at the interface, thus reducing the disparity between the magnitudes of the two different types of orientational order. For comparison with the case of $\alpha = 1$ (Figures 2(a) and 3(a)), Figures 6(a) and 6(b) show layer-wise variation of the two orders with ε_S at $\alpha = 0.1$. It is seen that the threshold value for the anchoring transition is now around 0.52 and the radius of the inner uniaxial core has diminished.

To examine the growth of the core region with uniaxial order as a function of changes in the splay constant, we show layer-wise variation of S_A as α is varied (Figure 5(b)). From this one can infer the typical size of the core sustaining uniaxial order and its dependence on splay elasticity. These results are plotted in Figure 5(c), showing a linear variation of the radius of the spherical inner uniaxial core with scale factor α. From these results, one can also plot the variation of the threshold values of ε_S needed to induce the anchoring transition, as a function of different scale factor values (α), and this is shown in Figure 5(d). It is also illustrative to compute the ^{2}H NMR spectra for the different values of α, at the fixed $\varepsilon_S = 1$, to see how the corresponding layer-wise

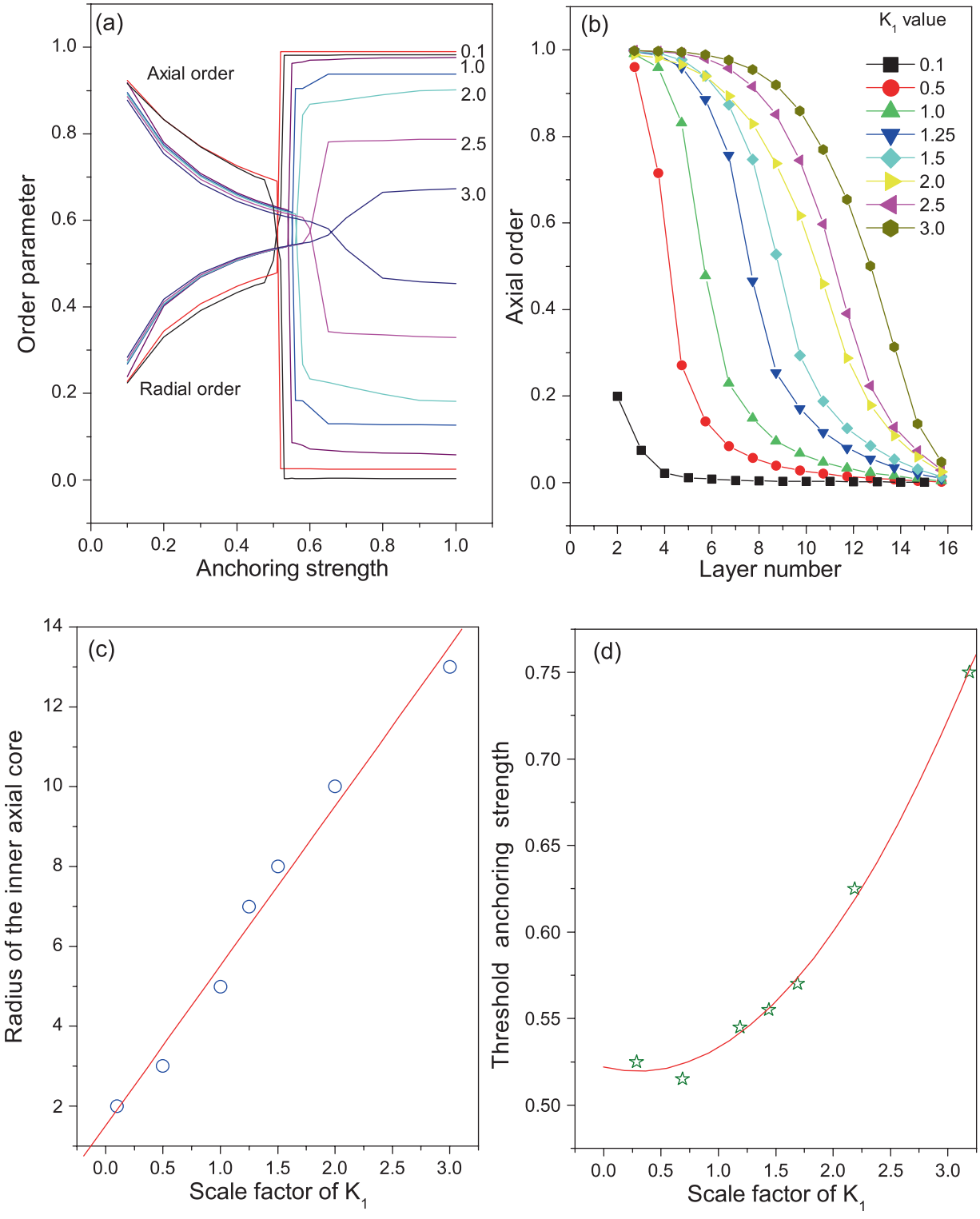

Figure 5. (a) Variation of the order parameters with anchoring strength for different scale factors, as indexed. (b) Variation of axial order for different K_1 with the layer number. (c) Radius of the inner axial order core with the scale factor. (d) Variation of threshold anchoring strength with scale factor.

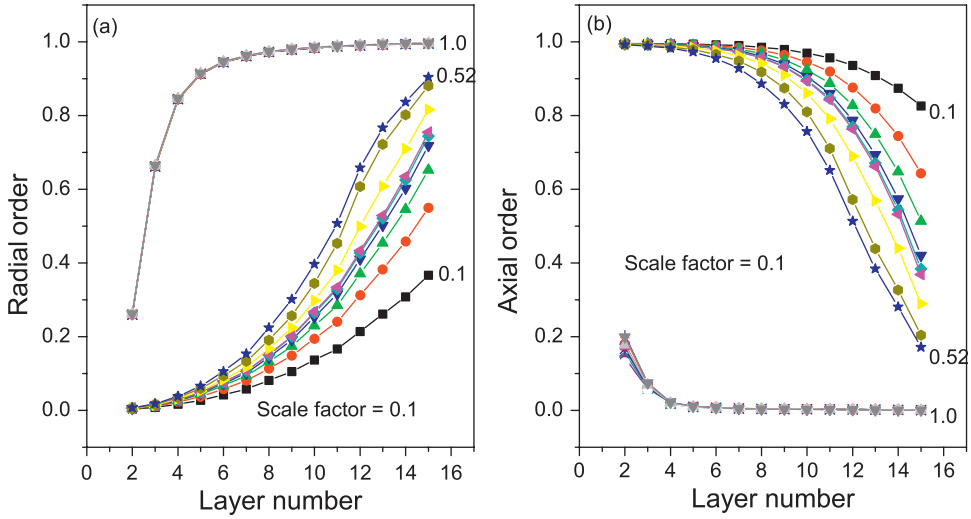

Figure 6. (a) Radial order for every layer for the scale factor 0.1 for different anchoring strengths. (b) Axial order for different anchoring strength for every layer at the scale factor 0.1 (the different plots correspond to different anchoring strengths ε_S, as indexed).

variation of the director field (Figure 5(b)) would react in an experimental situation, and this is shown in Figure 7. To look for possible hysteresis of this anchoring transition, given the abrupt changes induced by the anchoring strength, the simulations were repeated at $\alpha = 1$, by decreasing ε_S to zero starting from unity. The results are shown in Figure 8 and it is observed that there is a strong hysteresis associated with this anchoring transition. The transition to the original uniaxial state (at the lower anchoring values) could not be located precisely, and one can only infer that it should be somewhere between 0.1 and 0.0.

Finally, the applicability of this model depends on the dimension of the volume element Λ chosen to represent the average director field, and it was held fixed at 700 Å. To test limitations of this dimension on the results, simulations were also carried out (setting $\alpha = 1$) at two other values of Λ (70 Å and 7Å), and Figure 9 summarises the findings. At 70 Å (corresponding to the reduced temperature of 0.1), it could

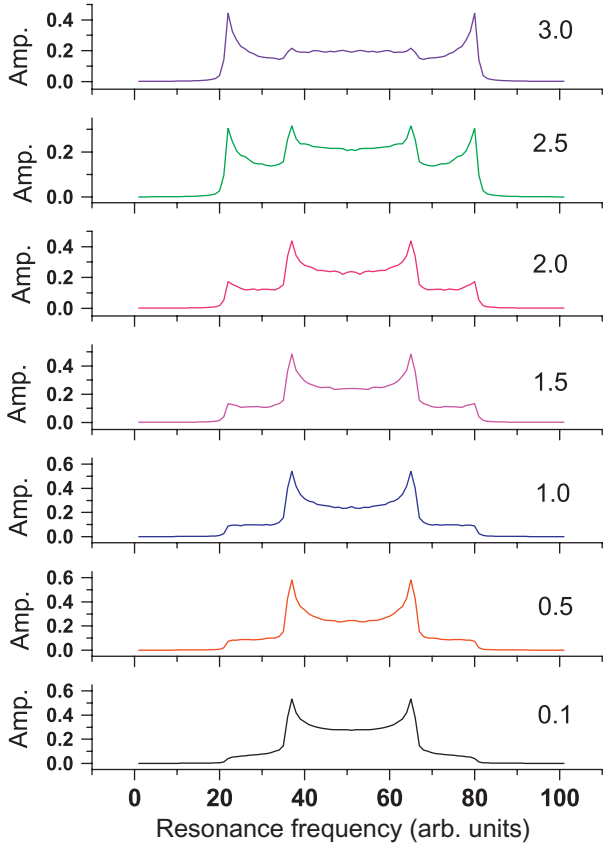

Figure 7. Simulated NMR spectra for various values of the scale factors.

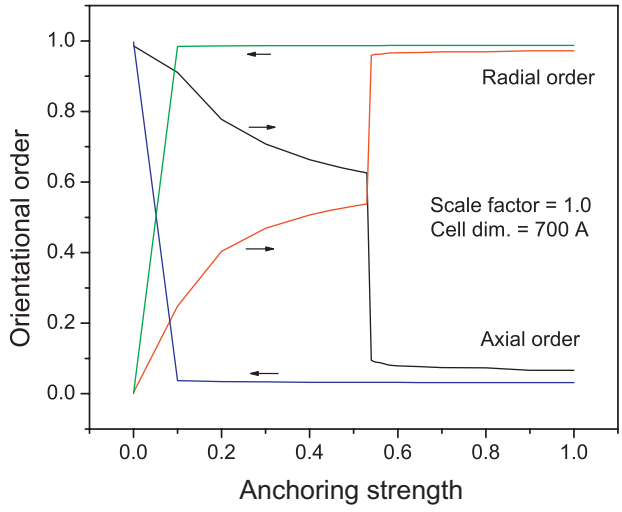

Figure 8. The hysteresis curve for cell dimensions (Λ) of 700 Å.

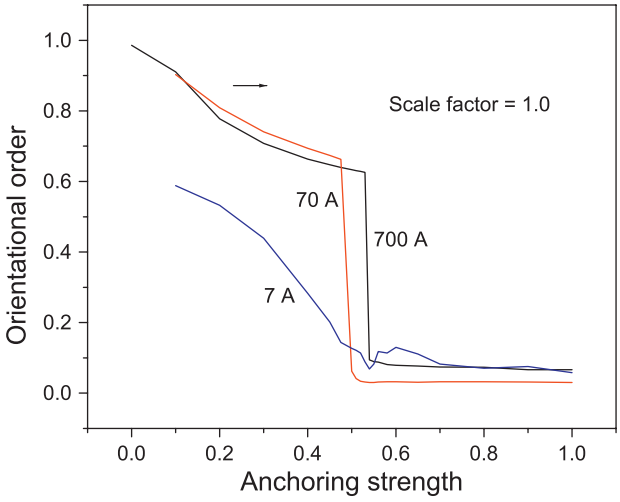

Figure 9. Variation of orientational order with anchoring strength for different cell dimensions.

be expected from the earlier work on planar hybrid films (*29*) that the volume element is too small to provide statically reliable representative director orientations (in statistical terms, the ensemble is collected at an unacceptably higher temperature), and any departures, if observed, were explained as being due to the effect of large director fluctuations. The present results thus show that at lower values of Λ the effect of director fluctuations is considerable, and the transition displays a shift in the threshold anchoring strength and also apparent weakening of the transition (Figure 9). The data at an even lower value shown in Figure 9 proves this point convincingly.

5. Conclusions

The liquid crystal micro-droplet is revisited with a different Hamiltonian model which permits explicit incorporation of the elastic properties of the medium, under certain conditions. We report here a structural transition in the director field, induced by tuning the anchoring strength at the spherical boundary. The layer-wise profiles of the two orders which distinguish the two phases, as well as their layer-wise fluctuations, provide an insight into the progression of this transition. The flexibility of this model is used to simulate the effect of assigning different splay properties of the medium (via the scale parameter), and the anchoring transition is studied as a function of the scale parameter, keeping other conditions the same. This affects both the anchoring threshold for the transition, as well as the extent to which the radial order could penetrate into the droplet. These effects can be conveniently gleaned by looking at ^{2}H NMR spectra (under rigid lattice conditions) which represent the variations of the director fields more transparently. The anchoring transition seems to be of strong first order leading to complete wetting, and it is reflected by the large hysteresis associated with this transition. This model is of course limited by the choice of the length scale connecting the volume element over which the local director is defined, and is effectively reflected in the MC simulation via the reduced temperature that is assigned during the simulation. These limits are also examined to see the effect of director fluctuations on the anchoring transition reported.

Acknowledgements

We thank the Center for Modeling Simulation and Design (CMSD), University of Hyderabad for providing its facilities, and GSP would like to thank DST-HPCF for the award of a research fellowship in the project (UH/CMSD/HPCF/2006-07).

References

(1) Grawford, C.P.; Zummer, S. *Liquid Crystal in Complex Geometries formed by Polymer and Porous Network*; Taylor & Francis: London, 1996.
(2) Drzaic, P. *J. Appl. Phys.* **1986**, *60*, 2142–2148.
(3) Chidichimo, G.; Arabia, G.; Golemme, A.; Doane, J.W. *Liq. Cryst*. **1989**, *5*, 1443–1452.
(4) Vaz, N.A.; Smith, G.W.; Montgomery, Jr., G.P. *Mol. Cryst. Liq. Cryst*. **1987**, *146*, 1–15.
(5) Doane, J.W.; Vaz, N.A.; Wu, B.G.; Zumer, S. *Appl. Phys. Lett.* **1986**, *48*, 269.
(6) Bowley, C.C.; Kossyrev, P.A.; Crawford, G.P.; Faris, S. *Appl. Phys. Lett.* **2001**, *79*, 9–11.
(7) Vilfan, M.; Zalar, B.; Fontecchio, A.K.; Vilfan, M.; Escuti, M.J.; Crawford, G.P. *Phys. Rev. E* **2002**, *66*, 021710.
(8) Doane, J.W.; Golemme, A.; West, J.L.; Whitehead, Jr., J. B.; Wu, B.G. *Mol. Cryst. Liq. Cryst* **1988**, *165*, 511–532.
(9) Golemme, A.; Zumer, S.; Allender, D.W.; Doane, J.W. *Phys. Rev. Lett.* **1988**, *61*, 2937–2940.
(10) Golemme, A.; Zumer, S.; Doane, J.W.; Neubert, N.E. *Phys. Rev. A* **1988**, *37*, 559.
(11) Chiccoli, C.; Pasini, P.; Semeria, F.; Zannoni, C. *Mol. Cryst. Liq. Cryst.* **1992**, *212*, 197.
(12) Amimori, I.; Priezjev, N.V.; Pelcovits, R.A.; Crawford, G.P. *J. Appl. Phys.* **2003**, *93*, 3248–3252.
(13) Kralj, S.; Zumer, S. *Phys. Rev. A* **1992**, *45* 2461.
(14) Zumer, S.; Doane, J.W. *Phys. Rev. A* **1986**, *34*, 3373.
(15) Vilfan, I.; Vilfan, M.; Zumer, S. *Phys. Rev. A* **1989**, *40*, 4724.
(16) Kralj, S.; Zumer, S.; Allender, D.W. *Phys. Rev. A* **1991**, *43*, 2943.
(17) Zumer, S. *Phys. Rev. A* **1988**, *37*, 4006.
(18) Onris-Crawford, R.; Boyko, E.P.; Wagner, B.G.; Erdmann, J.H.; Zumer, S.; Doane, J.W. *J. Appl. Phys.* **1991**, *69*, 6380–6386.
(19) Chiccoli, C.; Pasini, P.; Semeria, F.; Zannoni, C. *Phys. Lett. A* **1990**, *150*, 311–314.

(20) Lebwohl, P.; Lasher, G. *Phys. Rev. A* **1972**, *6*, 426.
(21) Berggren, E.; Zannoni, C.; Chiccoli, C.; Pasini, P.; Semeria, F. *Chem. Phys. Lett.* **1992**, *197*, 224.
(22) Pasini, P.; Chiccoli, C.; Zannoni, C. *Advances in the Computer Simulations of Liquid Crystals*; Kluwer: Dordrecht, 2000.
(23) Chiccoli, C.; Pasini, P.; Semeria, F.; Sluckin, T.; Zannoni, C. *J. Physique II* **1995**, *5*, 427.
(24) Berggren, E.; Zannoni, C.; Chiccoli, C.; Pasini, P.; Semeria, F. *Phys. Rev. E* **1994**, *50*, 2929–2939.
(25) Chiccoli, C.; Pasini, P.; Semeria, F.; Zannoni, C. *Mol. Cryst. Liq. Cryst.* **1992**, *221*, 19–28.
(26) Chiccoli, C.; Pasini, P.; Skacej, G.; Zumer, S.; Zannoni, C. *Lattice Spin Models of Polymer-dispersed Liquid Crystals in Computer Simulations of Liquid Crystals and Polymers*; Kluwer: Dordrecht, 2005; pp 27–56.
(27) Biscarini, F.; Chiccoli, C.; Pasini, P.; Semeria, F.; Zannoni, C. *Phys. Rev. Lett.* **1995**, *75*, 1803–1806.
(28) Chiccoli, C.; Pasini, P.; Feruli, I.; Zannoni, C. *Mol. Cryst. Liq. Cryst.* **2005**, *441*, 319–328.
(29) Le Masurier, P.; Luckhurst, G.; Saielli, G. *Liq. Cryst.* **2001**, *28*, 769.
(30) Murthy, K.P.N. *Monte Carlo Methods in Satistical Physics*; India: Universities Press, 2003.
(31) Gruhn, T.; Hess, S. *Z. Naturf.* **1996**, *A51*, 1.
(32) Luckhurst, G.; Romano, S. *Liq. Cryst.* **1999**, *26*, 871.
(33) Romano, S. *Int. J. Mod. Phys. B* **1998**, *12*, 2305.
(34) Schopohl, N.; Sluckin, T. *J. Physique* **1988**, *49*, 1097.